

F. -U. Gast · P. S. Dittrich · P. Schwille · M. Weigel
M. Mertig · J. Opitz · U. Queitsch · S. Diez · B. Lincoln
F. Wottawah · S. Schinkinger · J. Guck · J. Käs
J. Smolinski · K. Salchert · C. Werner · C. Duschl
M. S. Jäger · K. Uhlig · P. Geggier · S. Howitz

The microscopy cell (MicCell), a versatile modular flowthrough system for cell biology, biomaterial research, and nanotechnology

Received: 21 December 2004 / Accepted: 30 April 2005 / Published online: 27 July 2005
© Springer-Verlag 2005

Abstract We describe a novel microfluidic perfusion system for high-resolution microscopes. Its modular design allows pre-coating of the coverslip surface with reagents, biomolecules, or cells. A poly(dimethylsiloxane) (PDMS) layer is cast in a special molding station, using masters made by photolithography and dry etching of silicon or by photoresist patterning on glass or silicon. This channel system can be reused while the coverslip is exchanged between experiments. As normal fluidic connectors are used, the link to external, computer-programmable syringe pumps is standardized and

various fluidic channel networks can be used in the same setup. The system can house hydrogel microvalves and microelectrodes close to the imaging area to control the influx of reaction partners. We present a range of applications, including single-molecule analysis by fluorescence correlation spectroscopy (FCS), manipulation of single molecules for nanostructuring by hydrodynamic flow fields or the action of motor proteins, generation of concentration gradients, trapping and stretching of live cells using optical fibers precisely mounted in the PDMS layer, and the integration of microelectrodes for actuation and sensing.

F. -U. Gast (✉) · S. Howitz
GeSiM mbH, 01454 Grosserkmannsdorf, Germany
E-mail: gast@gesim.de
Tel.: +49-351-2695322
Fax: +49-351-2695320

P. S. Dittrich
Department Miniaturization, Institute for Analytical Sciences,
44139 Dortmund, Germany

P. Schwille
Institute for Biophysics/BioTec, TU Dresden, 01307 Dresden,
Germany

M. Weigel · M. Mertig · J. Opitz
Max Bergmann Center of Biomaterials and Institute of Materials
Science, TU Dresden, 01069 Dresden, Germany

U. Queitsch · S. Diez
Group Optical Technology Development and Bionanotechnology,
Max Planck Institute of Molecular Cell Biology and Genetics,
01307 Dresden, Germany

B. Lincoln · F. Wottawah · S. Schinkinger · J. Guck · J. Käs
Institute for Soft Matter Physics, Department of Physics and
Geosciences, University of Leipzig, 04103 Leipzig, Germany

J. Smolinski · K. Salchert · C. Werner
Department of Biocompatible Materials, Leibniz Institute
of Polymer Research and Max Bergmann Center of Biomaterials
Dresden, 01069 Dresden, Germany

C. Duschl · M. S. Jäger · K. Uhlig · P. Geggier
Fraunhofer Institute for Biomedical Engineering (Fh-IBMT),
10115 Berlin, Germany

Keywords Lab-on-chip · PDMS
microchannel · Microscopy · Hydrogel
valve · Microelectrodes

Abbreviations AC/DC: Alternating current/direct
current · AMPPNP: Adenosine 5'-(β,γ -
imido)triphosphate · ASE: Advanced silicon
etching · ATP: Adenosine 5'-triphosphate · cDNA:
Complementary (or copy) DNA · DNA:
Deoxyribonucleic acid · ECM: Extracellular
matrix · FCS: Fluorescence correlation
spectroscopy · FITC: Fluoresceine isothiocyanate · FN:
Fibronectin · FRET: Fluorescence resonance energy
transfer · GFP: Green fluorescent protein · Hz: Hertz
(s^{-1}) · kbp: Kilobase pairs · μ TAS: Micro total analysis
system · nDEP: Negative dielectrophoresis · nM:
Nanomol/liter · nN: Nanonewton · OD: Outer
diameter · PCB: Printed circuit board · PDMS:
Poly(dimethylsiloxane) · PMMA:
Poly(methylmethacrylate) · PNIPAAm: Poly(*N*-
isopropyl acrylamide) · POMA: Poly(octadecene-*alt*-
maleic anhydride) · PTFE:
Poly(tetrafluoroethylene) · RNA: Ribonucleic
acid · TIRF: Total internal reflection
fluorescence · UNF: Universal National Fine Thread

1 Introduction

The idea of a micro total analysis system (μ TAS) or lab on a chip (Manz et al. 1990, 1991) has led to numerous approaches to miniaturization in biochemistry, molecular biology, and cell biology. The use of a fluorescence microscope for the observation of biochemical reactions, the study of live cells using image processing, and the enrichment of cells by sorting are of special importance here. An already commercially available approach is the negative dielectrophoresis (nDEP) to hold single cells in place (caging), to turn, to view (e.g., using a confocal setup), and to sort them (Müller et al. 1999; Duschl et al. 2004). These perfusion systems already use clever ways, such as microsyringe pumps, to connect the flow cells to external macrofluidics; i.e., they consist of a stainless steel fluidic block containing an irreversibly bonded microfluidic system into which the tubes are plugged via O-ring gaskets.

Although perfusion cells for the microscope exist generally, they are often too large, with volumes of several 10 to more than 100 μ l. There is thus a growing demand for a low-volume microfluidic perfusion system that is ideally composed of discrete modules, most of which can be reused for a new application. An important aspect of this is a simple interface between the macrofluidic and the microfluidic world, preferably using standard connectors. If this is achieved, rapid prototyping is possible where the macrofluidic system stays the same and only the microfluidic chamber is exchanged.

Moreover, it is often desirable to take apart the microfluidic channel. For one, proper cleaning is easier when the cover can be removed. A fixed cover also lowers the flexibility of the system: one might wish to modify the coverslip surface by attaching chemically

reactive groups, biomolecules, or live cells before introducing it into the channel system, which is impossible with an irreversible setup such as gluing or anodic bonding at high temperatures. And in order to use other surfaces, the coverslip should be replaced without exchanging the entire chip, hence reducing consumable costs.

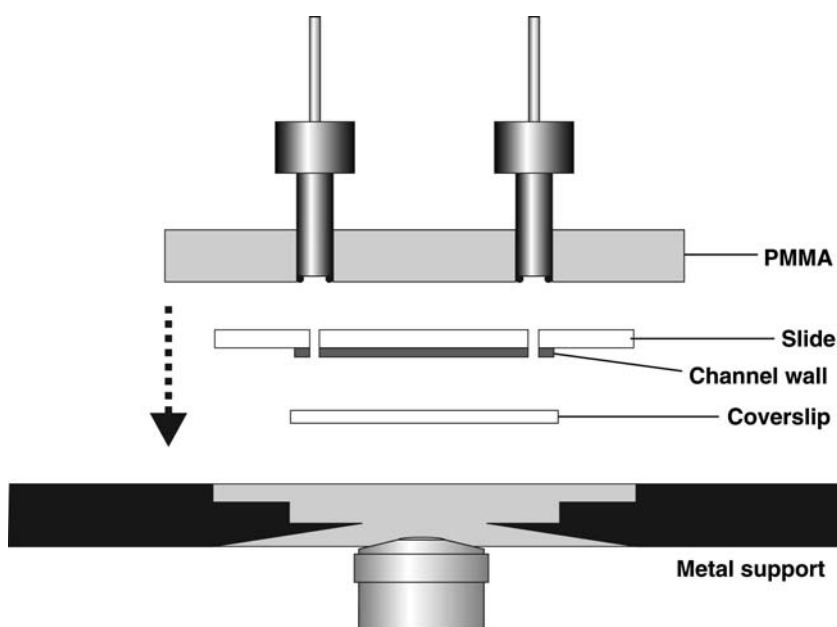
Here we present a microfluidic system that meets these requirements. It is based on a holder which is mounted in an inverted microscope and holds the chip by pressing together microchannel (usually PDMS) and coverslip. It also represents an interface between the microfluidic and the external macrofluidic system by providing standard connectors, for which we designed a novel PDMS casting station. Fluid flows are driven by computer-controlled syringe pumps and external or internal valves which can all be added in a modular way.

We further show experimental setups that have been realized in this system. The sheer number of applications already considered, tells one that many more applications can be expected in research areas as diverse as cell biology, biochemistry, biomaterial research, and nanotechnology.

2 Design and manufacturing of the microfluidic chip system

The idea of the MicCell is outlined in Fig. 1. It shows the assembly of the flow cell using a sandwich of a microchannel system (either completely from PDMS or, as shown here, using a glass substrate and microstructured walls) and a coverslip, held together by mounting it into a holder. This setup allows easy mounting and quick exchange of the channel system with alternative ones, while keeping constant all parts that connect to either

Fig. 1 Schematic drawing of the assembly of the microscopy chamber (not drawn to scale), as described in the text. Screws and springs for fastening and the adapter plate are not shown



the internal fluidics or to the microscope. Thus this system provides a customized flow cell with standardized macro-to-micro interface (fluidic connectors), which aids in rapid prototyping of the microfluidic system while easing the connection with external pumps.

In the normal setup, the flow cell incorporates a 150- μm thick standard coverslip (22 \times 22 mm), which seals a microchannel in a ca. 2-mm thick layer of poly(dimethylsiloxane) (PDMS), coined the “PDMS channel plate.” Casting of the PDMS layer is outlined in the following section. As regular coverslips without bore-holes are used, the PDMS channel plate must feature all inlet and outlet holes. The holder for the microchannel-coverslip sandwich consists of an aluminum support, which is directed to the microscope objective, and a lid from poly(methylmethacrylate) (PMMA), which holds all in- and outlets (Fig. 1) and, after assembling, is laid into an aluminum plate that adapts the microscopy cell to any type of inverted microscope (not shown). The experiments described in this publication were mostly performed on a Zeiss Axiovert 200M microscope.

In the standard setup, the PMMA cover holds up to four UNF (Unified National Fine Thread) fittings (Upchurch) for 1/16” OD PTFE (poly(tetrafluoroethylene), Teflon) tubes, but other geometries and more connections are possible. Inner tube diameters of typically 0.8 mm (but also values down to 0.3 mm) have been used here, smaller inner diameters can be realized using PEEK capillaries. Since almost the entire area of the soft PDMS layer with no extra gasket is used for sealing, the microchannel is watertight at fairly high flow rates, which are at least 150 $\mu\text{l/s}$ in a single channel of the typical channel dimensions (width: 3 mm; height: 50–100 μm), i.e. sufficient for all applications presented in Sect. 3, even without permanent attachment of the two layers by anodic bonding or gluing. If higher pressures are employed, sealing can be ensured by adjusting the pressure with which PDMS and coverslip are held together or by oxygen plasma treatment of PDMS (see Sect. 3.1).

2.1 Molding of the PDMS channel plate

Normally, PDMS molding is done by pouring a degassed solution of polymerizing monomer onto a master and curing. The channel formed at the master must then be sealed by a cover. The difficulty lies in the connection of the microchannels with outside tubes, for which no general solution exists.

We have replaced this awkward technique by a more reliable one. The channel is formed by injecting PDMS solution into a casting station with a syringe (Fig. 2a, b) containing the master (black) and capped by the PMMA lid mentioned above. In our case, the master is manufactured from silicon by photolithography and deep reactive ion etching (also called advanced silicon etching, ASE), for which the classical Bosch process (Lärmer and Schilp 1994) is employed. The masters are plasma-

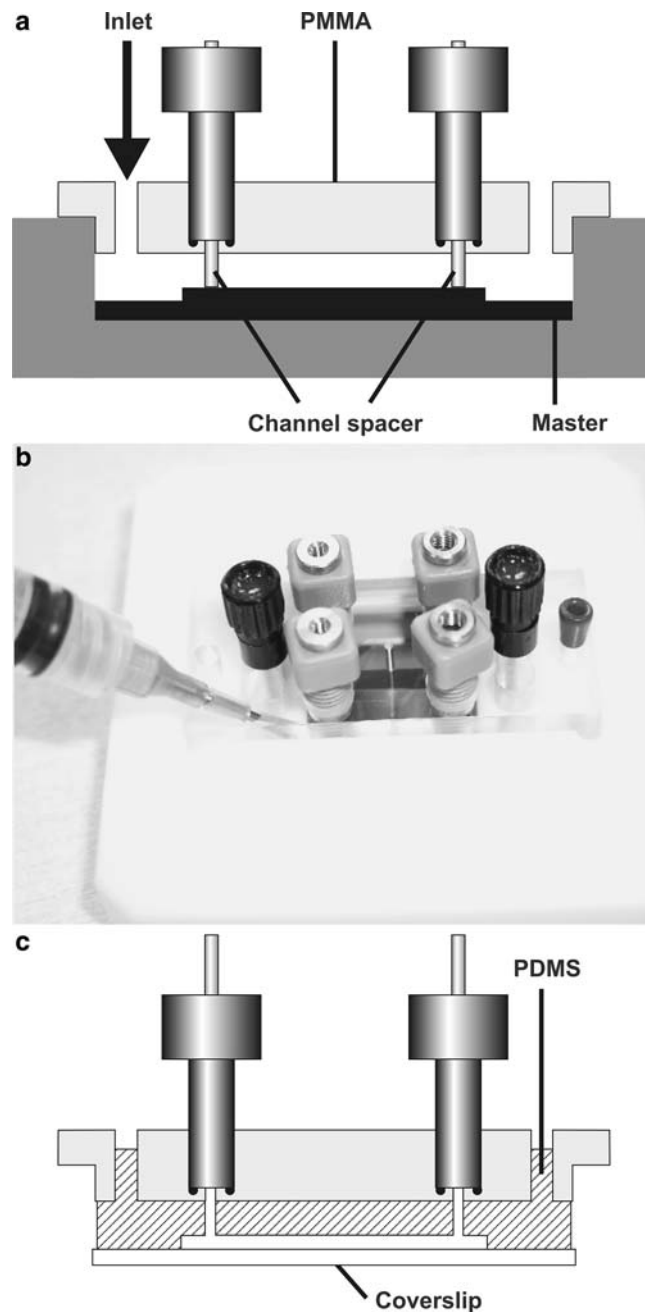


Fig. 2 Molding of the PDMS channel plate. **a** Schematic of the casting station; PDMS is applied through the inlet hole. **b** Casting of the PDMS gel; the four fittings screwed into the PMMA lid hold the channel spacers and are replaced by normal fittings in the assembled cell. **c** PDMS channel plate after demolding and capping with a coverslip. The sandwich shown is fixed on a metal support as in Fig. 1. The completely assembled MicCell is shown in Fig. 3b

coated with a PTFE-like material (C_xF_y) for easy demolding. A less expensive alternative for master fabrication, which is not shown here, is the patterning of one or more layers of photoresist on glass or silicon.

For casting, ten parts Sylgard 184 (Dow Corning) silicone elastomer are mixed with one part curing agent, degassed in an exsiccator for 30 min, and the mixture is injected into the molding station and cured for 45–

60 min at 80–100°C. As all inlet and outlet holes are located in the PDMS layer, they must be kept open during casting using “channel spacers,” i.e. tube fittings with a steel pin at the tip, (see Fig. 2a, b). These channel spacers are replaced by normal fittings when the MicCell is mounted (Figs. 2c, 3b). After curing, the PDMS channel plate, together with the PMMA lid, is taken out of the casting station such that the PDMS layer stays in contact with the PMMA cover, which then becomes the upper part of the holder in which the microchannel system rests (Fig. 2c). Due to the Teflon coating of the master and a slight shrinking of the gel, demolding is no problem. The slight shrinking affects neither the geometry nor the sealing of the microchannel.

The easy setup of the flow cell allows pre-coating of the coverslip (e.g., by spotting biomolecules or by growing cells on it before assembling) and the reuse of the cell by just exchanging the coverslip.

2.2 Other setups of the microsystem

If both top *and* bottom of the microchannel must be glass (either because biological components are sensitive to PDMS monomers even after extensive washing of the PDMS, or the system must be air-tight or microelectrodes must be present on both sides), the PDMS channel plate is replaced by a glass base (e.g., a slide with boreholes) on which channel walls are microstructured, as shown in Fig. 1. Structuring is most easily done using photoresist, e.g., SU-8 or dry photoresist films whose thickness can be adjusted by repeating the structuring process several times. To ensure watertight sealing, a gasket of silicone is applied on top of the photoresist walls, e.g., by screen printing (not shown). Sealing between the UNF fittings and the slide is achieved by O-rings, whereas the PDMS channel plate (see previous section) is self-sealing when pressed against the PMMA lid. The slide-polymer-coverslip sandwich is slightly less watertight than the PDMS channel plate, as the gasket is only placed at and around the channel walls, whereas in the PDMS channel plate, the entire area around the channel contributes to sealing.

As mentioned already, such a system can accommodate microelectrodes. We have devised a way to contact microelectrodes using contact pads present on both glass panes, (see chapter 3.6). All systems can also be manufactured in different sizes.

2.3 Reaction control by sample injection through a hydrogel microvalve

So far we have described a microchannel system that allows rapid prototyping while maintaining a standardized interface to the outside fluidics (without internal pumps, which improves the reliability of the system). If it is necessary to start and stop reactions, however,

valves are needed, which cannot be built into the PDMS layer.

Two possible solutions exist, an external and an internal one. An external selector (or distribution) valve (with several inlets and one outlet) can be used to switch between as many samples as input channels exist. These samples are then transported by a syringe pump (e.g., placed between selector valve and MicCell) into the microchannel. The advantage of an external valve is that it is robust, that it can be automated, and that it requires only a simple microchannel with one inlet and one outlet. If sharp boundaries between the injected fluids must be generated, however, an extra microfluidic input (i.e., a T-channel) is necessary. It is conceivable to use setups of either two syringe pumps upstream or one pump downstream of the MicCell, with or without additional external valves, but a complete discussion would go beyond the scope of this article. The disadvantage of external valves, however, is that large sample volumes are needed.

The other solution with minimal dead volume is a microfluidic valve. We have developed a hydrogel valve that contains particles of poly(*N*-isopropyl acrylamide) (PNIPAAm). This material is swollen when wet, but dehydrates above a certain transition temperature (thus opening the channel) and rehydrates when it is cooled down again, thus closing the valve up to a pressure of several bar (Richter et al. 2003, 2004). Depending on the degree of crosslinking, biocompatible transition temperatures around 20–40°C are realized (Richter et al. 2003, 2004). The switching temperature of the hydrogel injector valve type used here is 34°C, meaning that it is of the “normally closed” type, i.e., the injector inlet is shut at room temperature.

The currently smallest version of this valve is shown in Fig. 3a. Its upper layer (left panel) is a silicon substrate through which holes were etched. Its lower layer contains a cavity etched in silicon with similar through-etched holes. The cavity is filled with PNIPAAm particles (right panel). Platinum microelectrodes (insulated using silicon nitride coating) for heating (Fig. 3a, right) and temperature sensing (Fig. 3a, left) are structured on the silicon chips to control the actuator temperature and hence the hydration of the PNIPAAm actuator. Both silicon layers are flip-chip-assembled in a Fineplacer using glue, cured at 100°C, and then wire-bonded to a printed circuit board (PCB) that connects to an external electronic control unit. The chip unit is mounted inside a modified UNF fitting (sealing is achieved by O-rings), which is then screwed into one of the threads at the inlets of a branched microchannel (Fig. 3b).

In the easiest setup, the top side of the fitting containing the hydrogel valve is shaped like a funnel and sample solutions are pipetted into this cavity (Fig. 3b), but the hydrogel valve can also be connected to the sample via a tube. Different channel configurations exist to inject samples into the microchannel (Fig. 3c), the simplest being a T-junction (left panel). But as there is a small dead volume downstream of the hydrogel valve

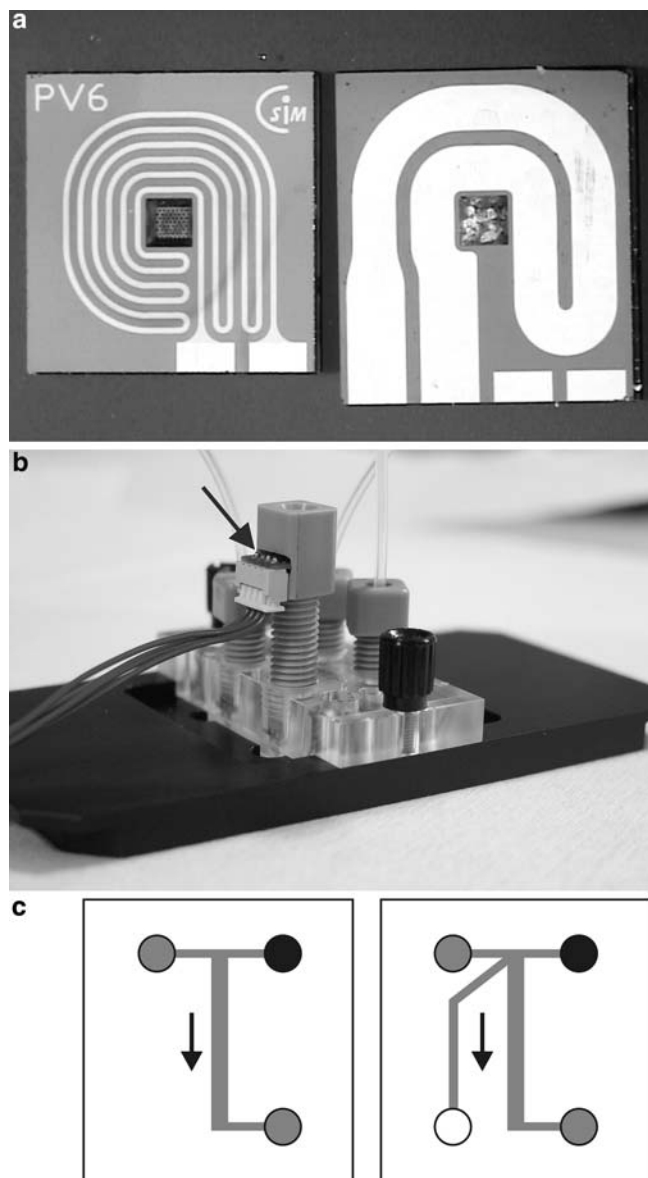


Fig. 3 The hydrogel microvalve, a modular switching device. **a** Small hydrogel chip before assembly. *Left*, silicon cover with through-etched holes and Pt temperature sensor; *right*, silicon base containing a heater and a cavity (with through-etched holes underneath) filled with hydrogel particles. Both parts are glued together, as described in the text. **b** Completely assembled MicCell consisting of PMMA lid, PDMS channel plate with K-channel and coverslip (under the PMMA lid), and metal support. It also contains inlet and outlet tubes plus an extra fitting with a funnel-shaped mold (*top*) and a built-in hydrogel valve (*arrow*). The electrical connections for heating and temperature sensing are plugged into the PCB of the hydrogel valve. **c** Possible channel geometries (T-type and K-type); *gray circles* represent inlets and outlets of the main channel, *black circles* represent inlets containing the microvalve, and the *white circle* represents an additional outlet to rinse the dead volume behind the hydrogel valve

(inside the “fitting” and in the microchannel just upstream of the T-junction), this area cannot be cleaned without affecting the main channel also. If the cleaning solution must not enter the main channel, another

channel downstream of the hydrogel valve is added, i.e., the T-junction and the two outward channels make up a “K-junction” (Fig. 3c, right panel). Hydrogel valves can normally be used only when the external syringe pumps are placed downstream of the flowthrough channel and thus aspirate (i.e., do not press) liquid.

Like all other active components, the hydrogel microvalve is controlled by software that allows all devices to be checked, priming of the channel system, electrical measurements, programming of fluidic processes (e.g., flow ramps), and external triggering (data not shown).

3 Applications

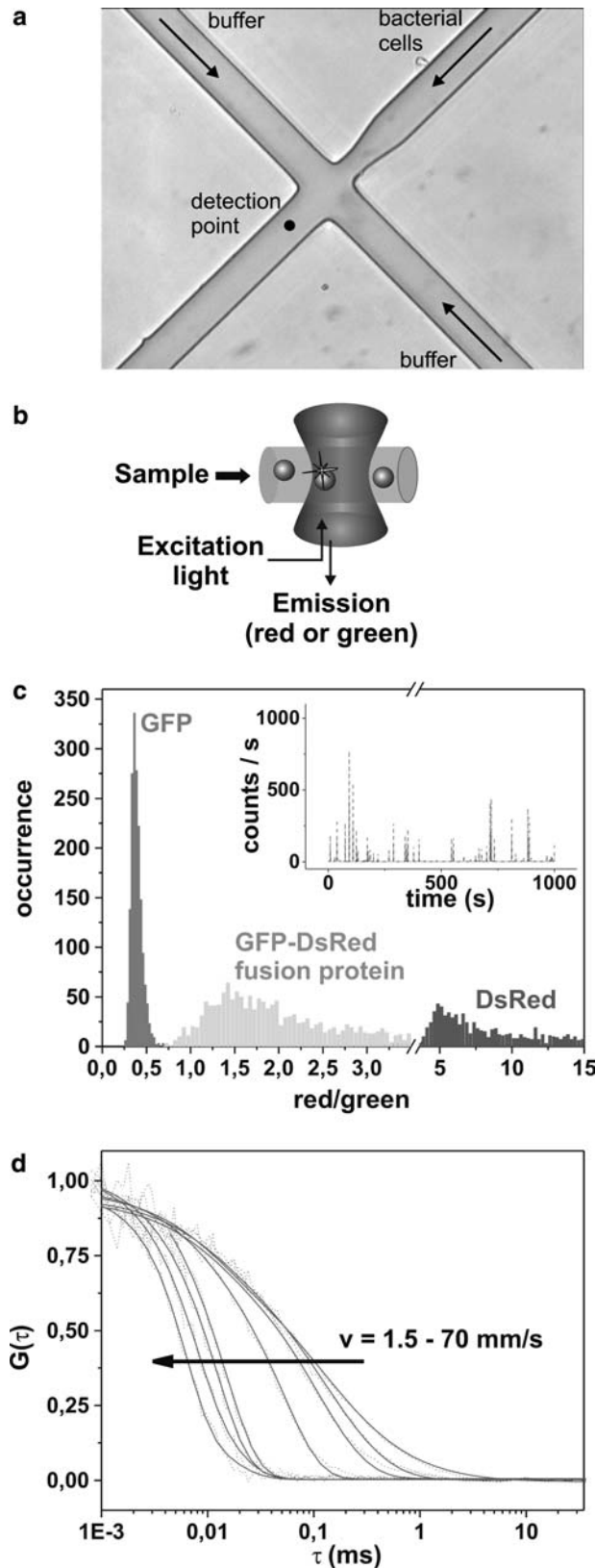
The analysis of large numbers of small particles, cells, organelles, and even macromolecules in search for novel and improved molecular or cellular functions (Georgiou 2001) is often realized by fluorescence-based techniques. The MicCell provides a versatile framework where computer-controlled external fluidic pumps are rapidly connected to a channel system that can be exchanged to adapt to numerous applications. To give an idea of the flexibility, this chapter lists diverse applications which have been performed in this system.

Fairly high flow speeds can be applied because the microfluidic system and the external syringe pumps are tightly connected with each other using standard fittings and O-rings, and because the sealing of PDMS on glass is good.

3.1 High-throughput cell screening using high-sensitivity multi-color fluorescence analysis

Automated detection and handling of particles and biomolecules and hence a cost-effective cytometer can be realized in small PDMS channel networks (Fu et al. 1999; Dittrich and Schwille 2003). Here PDMS and the covering glass plate are solidly bound after exposure to oxygen plasma, allowing high flow rates. To analyze a cell suspension, the sample is introduced into the middle channel of a crossed microfluidic system (Fig. 4a). The constant inflow from the two side channels into the main channel (all three channels are run with the same flow rate) generates a hydrodynamically focused sample stream where all cells line up and are detected in the microscope one after the other. Since analysis is completed in a millisecond, the concentration of cells and thus the throughput can be high.

The transparency of PDMS microstructures covered by a coverslip is compatible with a confocal fluorescence setup (Dittrich and Schwille 2003), allowing single-molecule detection, which is performed by the measurement of laser-induced fluorescence emitted from a tiny detection volume (approx. 1 femtoliter) at the center of the channel (Fig. 4b). By adequate optical filtering, two or more spectral wavelength regions are differentiated and spectroscopic parameters such as



color, or intensity, or efficiency of fluorescence resonance energy transfer (FRET) are determined (Fig. 4c).

While the cells are analyzed, the flow velocity (Fig. 4d) is controlled by fluorescence correlation

Fig. 4 Flow analysis of bacterial cells in a two-color confocal setup. The bacteria consist of three sub-populations expressing either green fluorescent protein (GFP), the red fluorescent protein DsRed, or a fusion protein in which both proteins are connected by a peptide linker (the latter can be differentiated by its specific ratio of red and green fluorescence). **a** Microscopic picture of the PDMS microchannel (channel $25 \mu\text{m}$ wide and $15 \mu\text{m}$ deep, constriction $15 \mu\text{m}$ wide). The main flow containing bacteria (coming from the upper right corner) is focused between two sheath flows such that all bacteria must pass the detection point (indicated by a black dot). **b** Measurement principle; emitted green and red fluorescence bursts of a sample passing the excitation light are analyzed. **c** Histogram showing the occurrence of red and green bursts (inset original data of green and red fluorescence = dashed and solid lines) whose ratio is taken to determine the bacteria type. **d** Analysis of the flow velocity by FCS. The decay time of the autocorrelation curves (dotted lines measured data, solid line curve fit), is inversely correlated to the flow velocity, as indicated by the arrow

spectroscopy (FCS), a technique that analyzes fluctuations in the fluorescence signal induced by single fluorescent molecules and particles entering and leaving the small detection volume (Madge et al. 1972; Eigen and Rigler 1994). The autocorrelation function of a fluctuating intensity signal, $G(\tau)$, specifies the similarity between a data point with a point measured after a delay time, τ ; of course $G(\tau)$ decays from a maximum value at $\tau \rightarrow 0$ to zero for large τ . The characteristic decay time corresponds to the average residence time of the fluorescent particles in the detection volume and hence can be used to derive their average velocity. This could be used to analyze flow velocity profiles in microchannels. For the measurement of the bacteria, we have used flow velocities of up to 300 mm/s (corresponding to a flow rate of ca. $8 \mu\text{l/min}$ in each channel). Due to the plasma treatment of the PDMS and hence stable binding of both materials, the flow cell was watertight up to a flow of $80 \mu\text{l/min}$ per channel. Typically, experiments were performed at a flow velocity of 5 mm/s in the channel center, corresponding to a flow rate of $1 \mu\text{l/h}$ in each channel.

The microfluidic setup presented here opens fascinating prospects for the screening of large populations, but also for the detection of rare events at low concentrations (Eigen and Rigler 1994). Since the optical setup allows the detection of weak signals, it is not limited to cells or particles; the analysis of single fluorescent macromolecules, e.g., the investigation of reaction kinetics (Lipman et al. 2003; Dittrich et al. 2004), is also feasible. Intermolecular reactions could be studied by caging all reactants in reaction chambers (Dittrich et al. 2005).

3.2 Nanostructure fabrication by manipulating single molecules in the hydrodynamic flow

The bottom-up fabrication of artificial nanostructures makes use of molecular recognition and self-assembly (Braun et al. 1998; Mertig and Pompe 2004). Deoxyribonucleic acid (DNA), in particular, has been used as a building block, because the specific Watson-Crick base

pairing allows the build-up of artificial supramolecular structures by programming all intra- and intermolecular interactions (Seeman 1996; Yan et al. 2003). DNA is also a template for metallization into wire-like assemblies for nanoelectronics (Richter et al. 2001; Mertig et al. 2002; Yan et al. 2003). Here we show the integration of single DNA molecules into microelectronic contact arrays by site-specific immobilization and manipulation in the flow.

In most cases, end-specific attachment of a DNA molecule to a micro-contact pad requires functionalization of both contact pad surface and DNA end. One can, e.g., hybridize the sticky ends (if present) of a large double-stranded DNA to complementary oligodeoxyribonucleotides which were immobilized on gold contacts via a thiol group (Braun et al. 1998), or attach DNA via an Au-biotin-streptavidin-biotin-DNA bridge (Zimmermann and Cox 1994). Here we use electrostatic bonding between negatively charged DNA (due to its phosphate groups) and positively charged amino groups, which does not require DNA modification. Small contact pads, fabricated by vapor deposition of Au through a mask onto a glass substrate, are amino-functionalized with cysteamine (Maubach et al. 2003). Figure 5a shows a series of images where a diluted solution of fluores-

cently labeled λ -phage DNA (48.5 kbp, corresponding to a contour length of 16.5 μm) flows across the contact array and multiple DNA molecules are bound. We determined a pH optimum of 8.0 for the pH-dependent (Allemand et al. 1997) binding of DNA to cysteamine-coated gold pads. Simultaneous binding of both ends of one DNA molecule occurs rarely compared to the binding of single ends, as the molecules are stretched after binding.

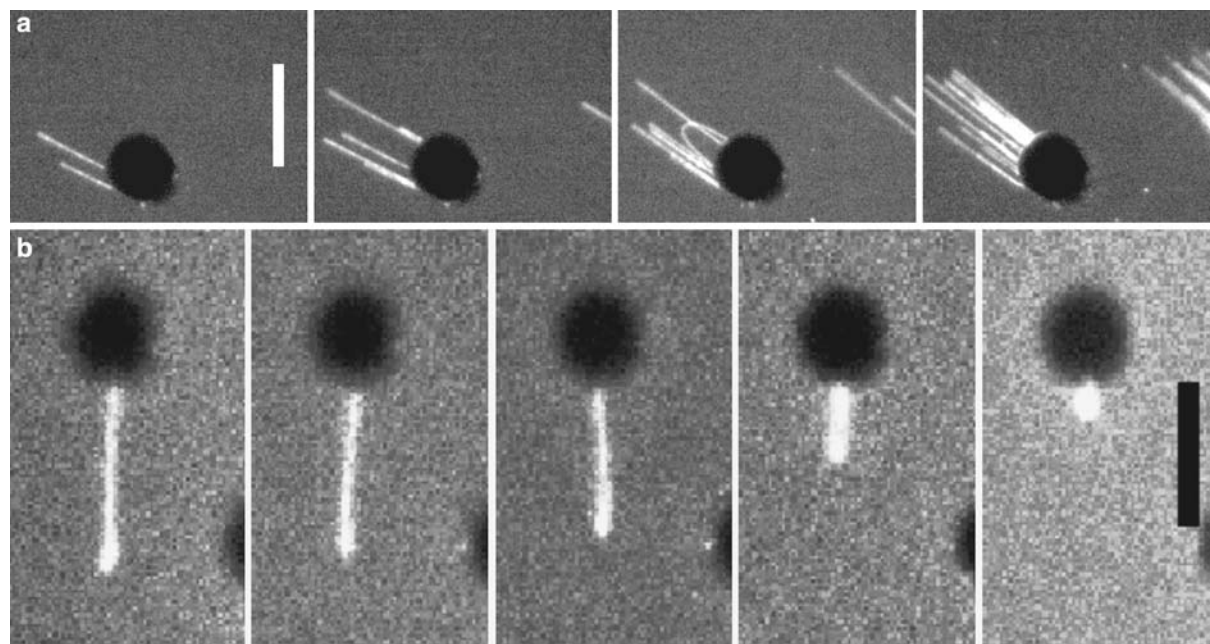
The MicCell can control the degree of stretching of the anchored DNA molecules by adjusting the flow velocity (Wirtz 1995; Larson et al. 1997), as shown in Fig. 5b. At the highest flow rate tested, the apparent DNA length reaches 83% of the contour length. Brownian motion of the free DNA end can be seen at constant flow (data not shown). The free end of the molecule appears lighter as the mid-segment of the DNA, indicating that the free end is still coiled (Wirtz 1995); this effect increases with decreasing DNA length. By changing the flow direction (either by reverting the flow or by using different inlets and outlets), the direction of the DNA changes and hence the controlled bridging of certain contact pads by DNA molecules becomes feasible (Mertig and Pompe 2004).

The laminar flow in a microchannel results in different flow velocities in the center and at the edges of the flow channel. This velocity profile can be determined by tracking the trajectories of small polystyrene beads at different XY -positions and at different focal planes (data not shown).

Fig. 5 Fluorescence microscopy images of the binding and stretching of λ -DNA molecules stained with YOYO-1 (Molecular Probes), appearing as light lines. Experiments were performed in the center of a 500 μm deep channel. The scale bars represent 10 μm . **a** λ -DNA binding to a cysteamine-functionalized gold dot (black) under constant diagonal hydrodynamic flow (10 $\mu\text{l/s}$). **b** Images of a λ -DNA molecule attached with one end to a gold contact at flow rates that decrease from 10 $\mu\text{l/s}$ (leftmost panel) to 0.5 $\mu\text{l/s}$ (rightmost panel); the actual flow velocity at the surface is much smaller due to the laminar flow profile in the channel

3.3 Handling of motor proteins in microflow channels

Motor proteins perform a variety of tasks inside cells, such as the transport of vesicles and the separation of chromosomes. There is currently much interest in their



nanobiotechnological application, as they can be used to transport and manipulate nano-objects in a cell-free environment. This idea is intriguing because such machines, while being in the nanometer range, are robust and can work in parallel with high energy efficiency.

Two setups to study motor proteins *in vitro* (so-called motility assays) exist. In the gliding assay, the motors are immobilized on a surface and the filaments glide over the assembly (Fig. 6a). In the stepping assay, the filaments are laid out on the surface where they form tracks for the motors to move along (Fig. 6b). In both cases, the movement is observed under the light microscope using fluorescence markers or high-contrast brightfield techniques. Variations on these assays have been used to reconstitute motility on various filaments (actin filaments, microtubules, DNA, RNA).

Using the kinesin-microtubule transport system, the gliding assay has provided data on the directionality, speed, and force generation of purified molecular motors (reviewed by Scholey 1993; Howard 2001). First nanotechnological applications have been demonstrated and include the transport of streptavidin-coated beads *in vitro* (Hess et al. 2001), the measurement of forces in the piconewton range (Hess et al. 2002a), the imaging of structured surfaces (Hess et al. 2002b), and the motor-driven transport and stretching of individual DNA molecules that were attached to microtubules (Diez et al. 2003).

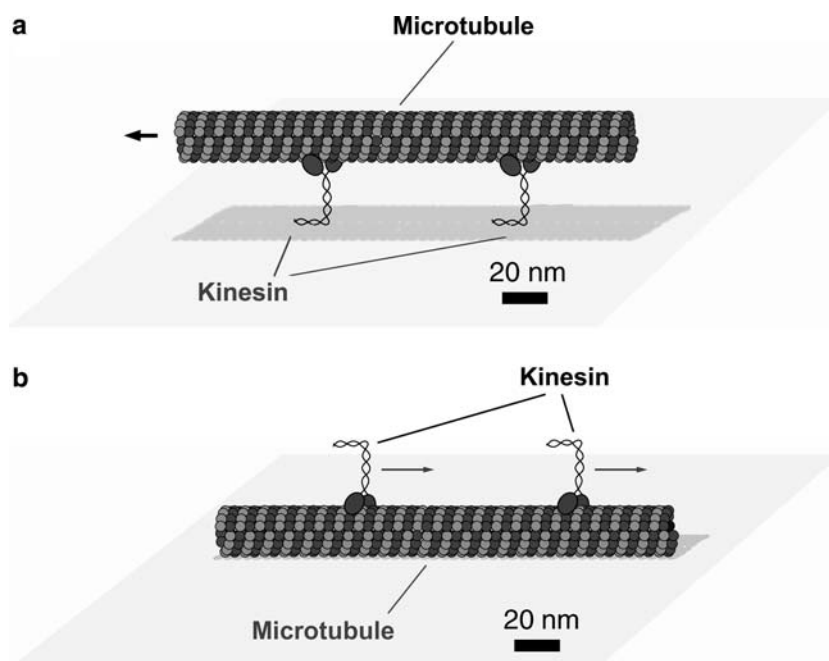
The MicCell microperfusion system is of extreme value for these studies. Using a computer-controlled flow system and a hydrogel injector valve, the activity of the enzymes can be started and stopped by controlled supply of ATP (adenosine 5'-triphosphate) or inhibitors and flow fields can be used to apply forces onto the

motors or filaments. The in-focus imaging need not be stopped during flow application, allowing full observation of the biophysical effects with high time resolution.

In order to control the gliding movement of microtubules on a kinesin-coated surface, hydrodynamic flow (Stracke et al. 2000; Prots et al. 2003) has already been applied to direct the motion of gliding filaments. Microtubule motility could be started and stopped by manipulating the ATP concentration (Böhm et al. 2000; Hess et al. 2001). Figure 7 demonstrates that gliding motility assays can easily be performed in our flow-through system and that the spatio-temporal control over the microtubule movement is readily achieved. Figure 7a shows the alignment of motile microtubules that originally migrate over the surface in random direction, but “follow” the hydrodynamic flow field once it is switched on.

Figure 7b shows the starting and stopping of motor activity by either supplying ATP (the normal substrate) or AMPPNP (adenosine 5'-(β,γ -imido)triphosphate, a non-hydrolyzable ATP analog) into the flow cell, respectively. The microtubules repeatedly resume movement upon ATP addition. The sharp transition between movement and resting indicates the timely operation of the MicCell system. The short delay of the onset of motility after ATP addition is caused by the rather slow exchange of bound AMPPNP by ATP reported by Schnapp et al. (1990). In these experiments, hydrodynamic flow has only been applied during the phases of nucleotide exchange in the chamber (about 10 s duration). The majority of the data points for the gliding velocities have thus been recorded in the absence of any hydrodynamic flow. However, in other experiments where ATP-containing motility solution was

Fig. 6 Principal setups to study motor proteins *in vitro*. **a** Gliding assay; **b** stepping assay



continuously flown through the perfusion chamber, we did not find any significant influence of the flow onto the gliding velocity (just the direction of gliding).

The MicCell will be beneficial for the study of motor proteins in the stepping motility configuration. By combining it with highly sensitive fluorescent imaging based on total internal reflection fluorescence (TIRF), we aim to bind kinesin or kinesin-like motors to immobilized microtubules in the absence of ATP and to study their first steps after ATP addition. A further field of development will be the directed movement of microtubules or motor proteins to which DNA molecules are bound to aid the bottom-up fabrication of nanowire networks (see also Sect. 3.2 and Diez et al. 2003).

3.4 Generation of protein concentration gradients

Cellular adhesion, migration, and growth are mediated by proteins and other components of the extracellular matrix (ECM), including collagen, fibronectin (FN), heparan sulfate, and various growth factors. One of the ECM molecules, FN, a 450-kDa glycoprotein, was chosen to generate surface-bound protein gradients to

study the impact of immobilized ECM at varying concentrations.

Lateral surface gradients can be prepared by diffusion-based principles, density gradients, radiofrequency plasma treatment, localized polymer hydrolysis (Ruardy et al. 1997), and by laminar flow of protein solutions in microchannels (Li Jeon et al. 2000; Dertinger et al. 2001, 2002). The MicCell turned out to be ideal to generate protein gradients in the laminar flow, which is based on the reduced mixing in a microchannel as compared to the turbulent mixing in large channels. Thus if solutions of different concentrations are merged using the “tree” of microchannels (mixer) shown in Fig. 8a, a well-defined concentration gradient perpendicular to the flow direction and across the channel width is stably established. In the first experiment of this kind, three syringe pumps were used to pump the three solutions into the microchannel (experiments with two inlets are under way).

This gradient flow was utilized to deposit FN onto a reactive polymer substrate. Coverslips were first coated with thin films of poly(octadecene-*alt*-maleic anhydride) (=POMA) (Pompe et al. 2003), and then attached to the PDMS microchannel shown in Figs. 8a–c. The two-dimensional FN gradient was formed on the POMA

Fig. 7 Gliding microtubule motility assays in the MicCell. **a** Alignment of migrating microtubules in the flow. *Left panel* random movement before flow application (movement direction indicated by *arrowheads*, microtubules *without arrowhead* are stationary); *right panel* directed movement of microtubules approximately 2 min after starting a flow field (indicated by the *large arrow*) with $0.5 \mu\text{l/s}$. **b** Starting and stopping of microtubule motility upon application of ATP or AMPPNP (1 mM each in buffer) into the flow channel, respectively (velocity averaged over ten microtubules)

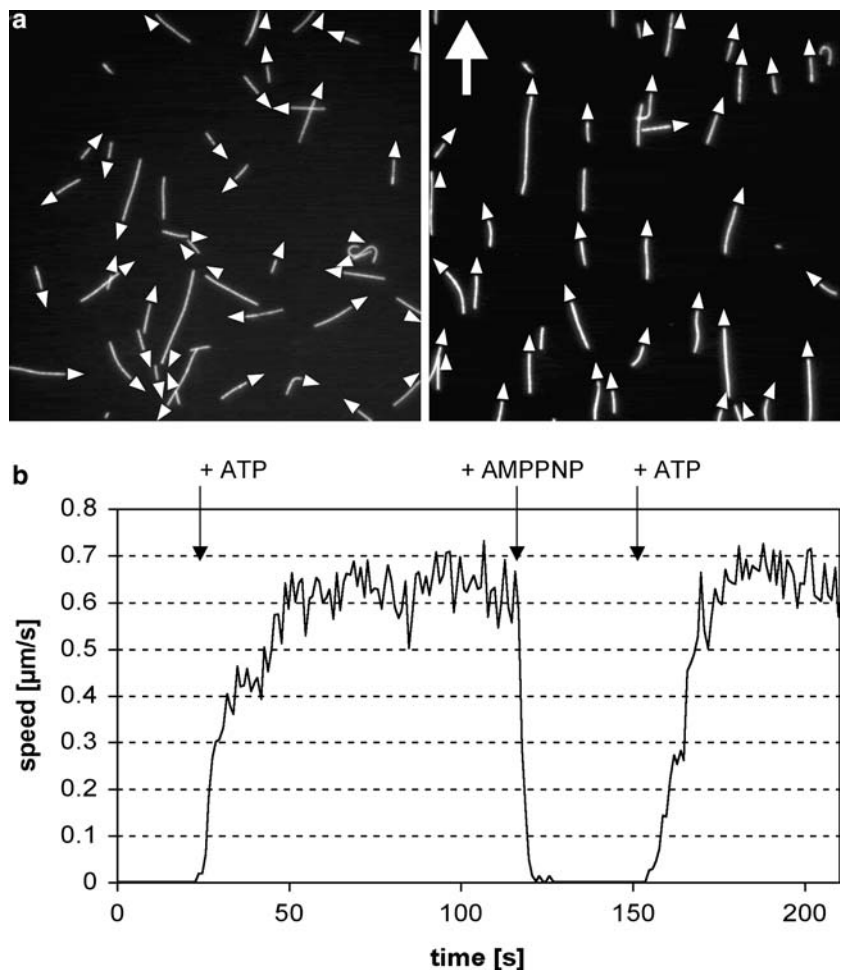
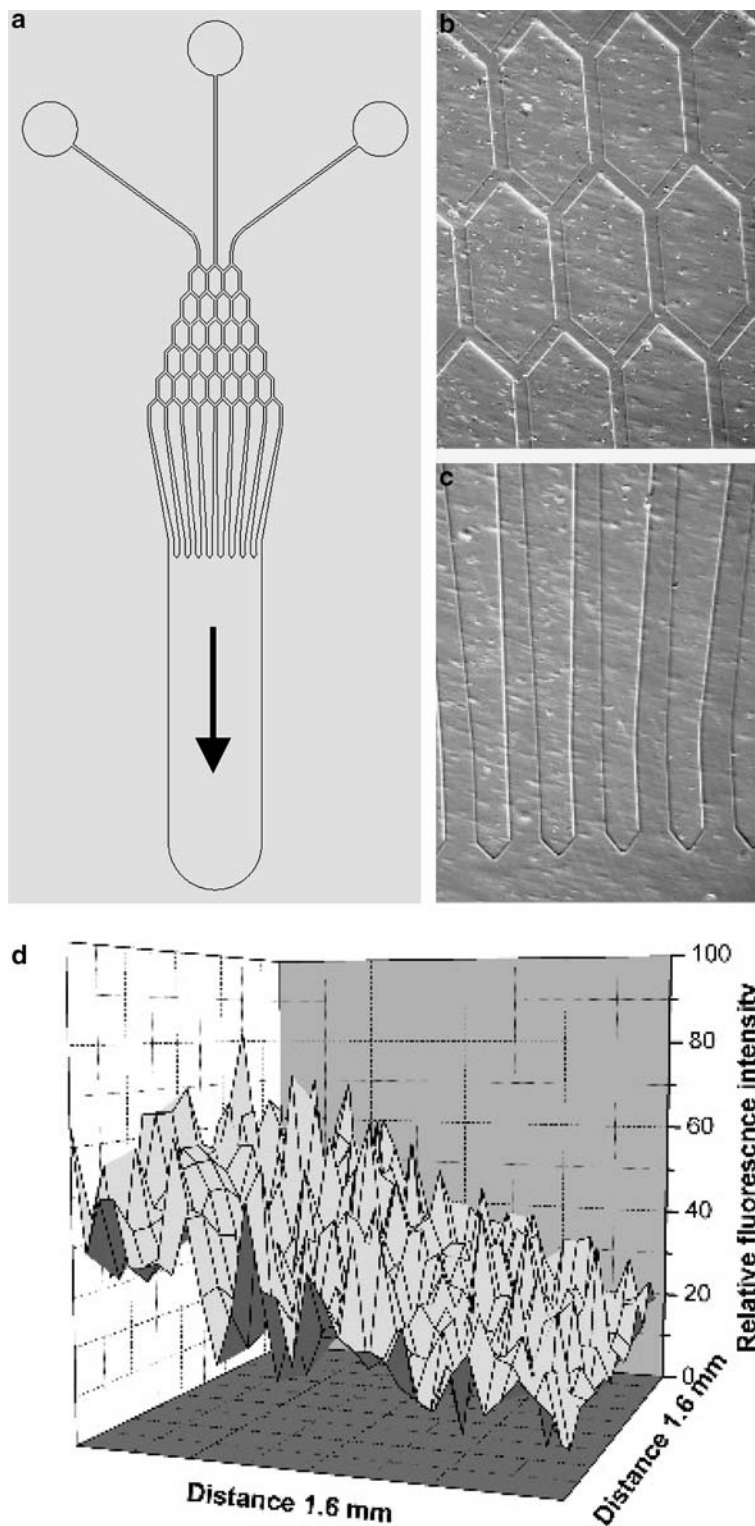


Fig. 8 Generation of lateral concentration gradients. **a** Drawing of the gradient-forming “channel tree,” three inlets guide protein solutions with different concentrations into the mixer, producing several streams of graded protein concentrations that are combined in a 1.6 mm wide channel. The flow direction is indicated by the *arrow*; the gradient is formed perpendicular to this direction. **b, c** Detailed views of the central and the exit region of the micromixer; PDMS channels are 50 μm wide and 50 μm high. **d** Diagram of the gradient of surface-bound fluorescent FN on POMA as determined by confocal laser scanning microscopy of a 1.6 \times 1.6 mm area that was covered by the gradient in the channel. The gradient was formed from three solutions containing 25, 12.5, and 0 $\mu\text{g}/\text{ml}$ FN in phosphate-buffered saline and the total flow (sum of all three inlets) was kept at 30 $\mu\text{l}/\text{s}$



coating from the flowing solution after connecting the three inlets of the MicCell to reservoirs with different protein concentrations and FN was immobilized on the POMA coating upon application of the flow. An example of the resulting gradient is shown in Fig. 8d.

Experiments are ongoing to test various polymer pre-coatings, the immobilization other ECM

components, gradient mixers with a finer grid for smoother gradients, and the generation of two-dimensional concentration landscapes by turning the coverslip by 90° between two runs, roughly as described by Cesaro-Tadic et al. (2004). Finally, the functionalized substrates will be implemented in cell-based assays using the MicCell platform.

3.5 Integration of optical fibers into the PDMS layer: an optical cell stretcher with microfluidic integration for cell characterization and sorting

A new technique for single-cell measurements called the “optical stretcher” is a laser trap consisting of two divergent, counter-propagating laser beams guided by single-mode optical fibers (Guck et al. 2001). The transfer of momentum from the light to the cell surface leads to a stable trapping configuration at low laser power. At higher laser powers of 0.8–1.5 W, the two lasers can also deform cells (Guck et al. 2000), enabling the determination of the viscoelastic signature of the cytoskeleton (Elson 1988; Schinkinger et al. 2004; Wottawah et al. 2005). This can be used as a cell marker, as cancer cells are softer than non-malignant cells and stem cells are softer than differentiated cells (Guck et al. 2005).

For a correct functioning of the microfluidic optical stretcher, the two 80 μm thick optical fibers must be aligned to at least 3 (preferably 1) μm , which is challenging given that PDMS is a rather flexible material. We have solved this problem by structuring a funnel-like recess for the optical fibers in the PDMS layer (Fig. 9a) of about the same width and using a mechanical feeder to pre-align and feed the fibers into the microsystem under microscopic control. Channel widths were 3 mm, narrowed down to about 250 μm at the trapping/detection zone; the distance between the fibers and the flow channel was 100–200 μm . In this fiber-integrated microfluidic system, the cells could be serially trapped, deformed, and their mechanical properties determined (Fig. 9b).

While many techniques exist to probe viscoelastic properties of cells (Huang et al. 2004; Van Vliet et al. 2003), the optical stretcher is unique in that its nature as an optical trap lends itself to automation (Lincoln et al. 2004); i.e., a larger, unbiased sample can be measured, the number of preparations needed to attain a desired cell number is reduced, and medium swapping and cell sorting, e.g., by applying nDEP (Müller et al. 1999; Duschl et al. 2004) or laser tweezers (reviewed by Grier 2003), can be realized. A number of microfluidic devices have been recently developed to facilitate single-cell experiments (Andersson and van den Berg 2003), but the optical stretcher is the first to assess the cells’ deformability.

Applications of this technique are vast. Even though the method is nonspecific and the effect is in the range of a few percent, it is fast and absolutely reliable when using proper image processing. Thus cancer cells can be detected without need for biopsy; fine needles or cytobrushes would collect enough cells. Stem cells can be isolated from heterogeneous populations. This high-throughput system requires no labeling or mechanical contact, leading to high viability of the sorted cells while leaving them unaltered for further therapeutic use. Additionally, cells can be monitored over time for viscoelastic changes during differentiation, cell cycle, or in

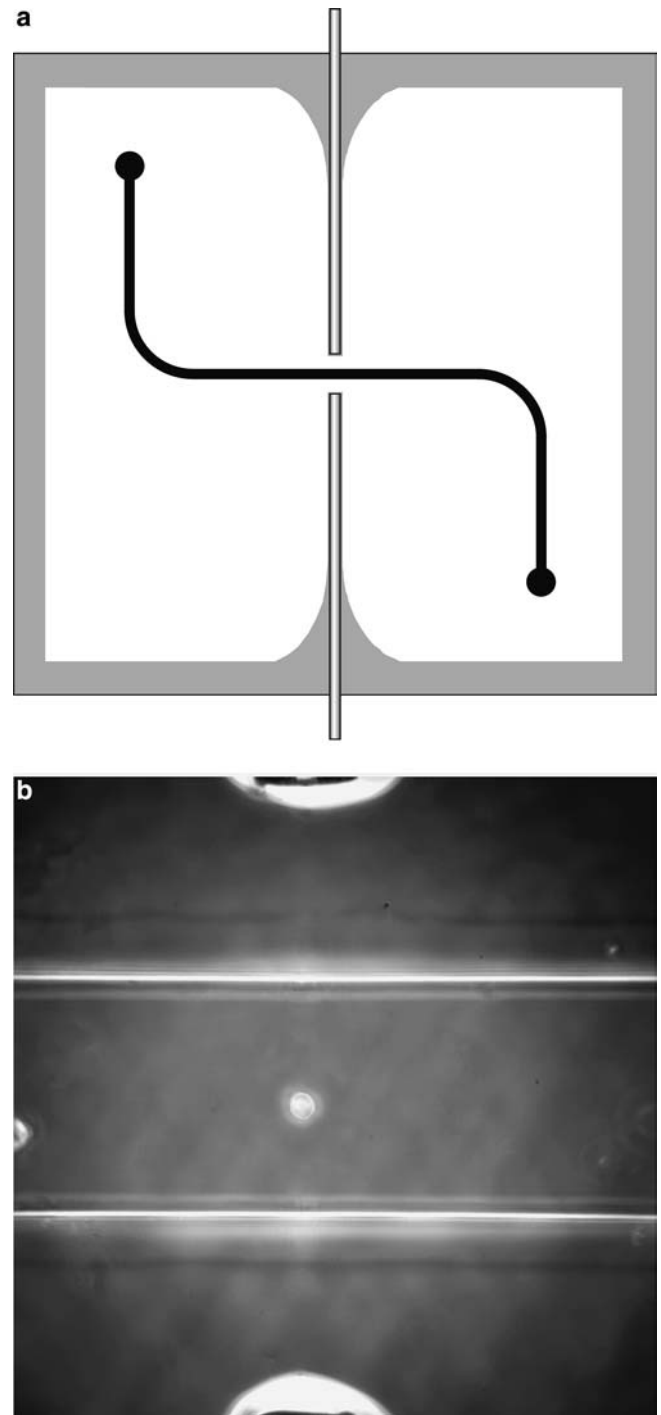
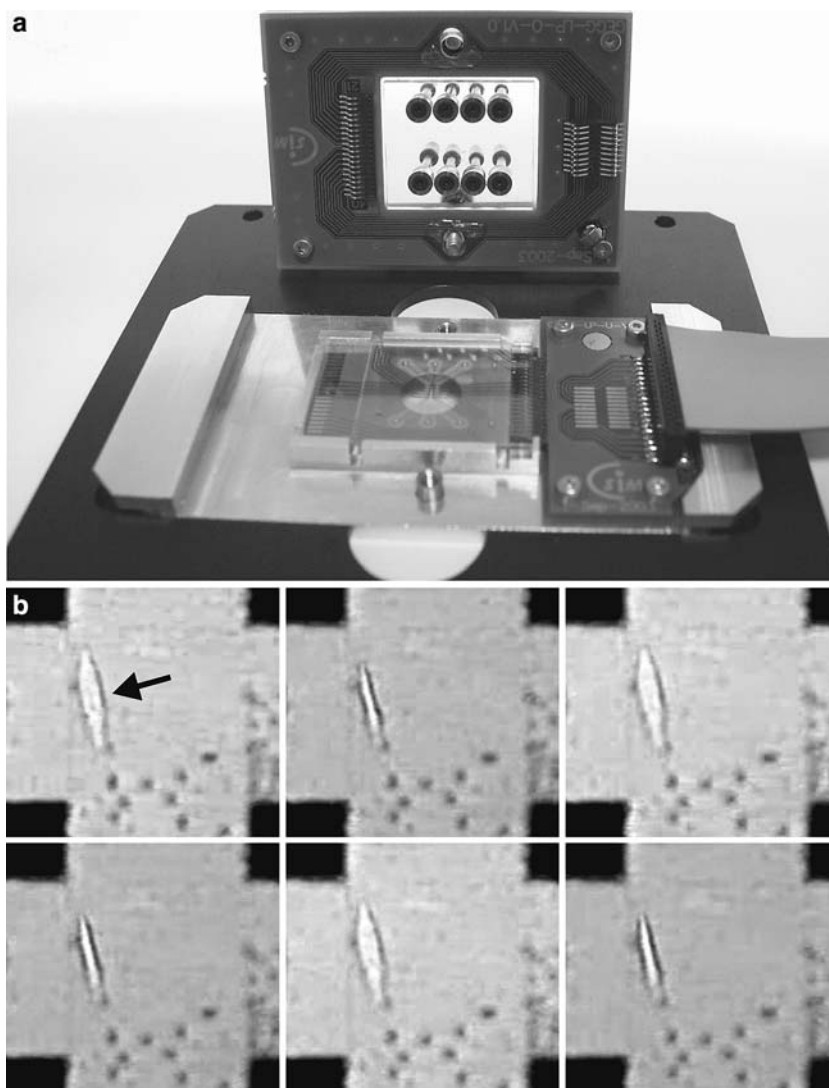


Fig. 9 Integration of optical fibers into the MicCell system as exemplified by the optical stretcher. **a** Schematic of an optical stretcher with a single channel (black) and two aligned optical fibers (gray) used for trapping and stretching; the PDMS layer is white. If sorting by radiation pressure is needed, an optical fiber and another exit channel are added downstream of the detection point. **b** Enlarged picture of the detection region of an unbranched microchannel (as in **a**) with a trapped human promyelocytic leukemia (HL-60) cell. The two aligned optical fibers in their PDMS guide channels are seen right at the *top and bottom* of the picture. Stretching is too small to be seen at this magnification

Fig. 10 Integration of electrodes into the MicCell to generate pH waves for forisome actuation. **a** Chamber prototype, mounted and laid into the adapter plate, with open cover. Electrodes are structured on both sides of the microchannel. PCBs with spring contacts are placed above and below the glass substrates; the ribbon cable seen on the right is connected to the input voltages. A similar setup can be used for nDEP. **b** A forisome (arrow) between four planar platinum microelectrodes (black areas in the corners) on a glass substrate as seen by transmission light microscopy. A pH change and hence a forisome response is induced using an AC/DC generator by activation of the two electrodes in the top left (anode) and bottom right corners (cathode) at $2.25 \text{ V}_{\text{rms}}$ and approx. 0.1 Hz . Images were taken after 0, 7, 13, 15, 22, and 28 s



response to drugs. Due to its noninvasive nature, the optical stretcher might become a standard component of a lab-on-chip that could be combined with any other single-cell technique.

3.6 Electrodes in the MicCell: electrotitration to drive pH-dependent contraction and expansion of ATP-independent mechanically active polymers

The integration of electrodes dramatically expands the capability of the MicCell. It is, however, incompatible with PDMS, but requires a hard surface like glass. If electrodes are present on only one side, the channel system can still be made of PDMS and microstructuring of electrodes (e.g., of transparent material such as indium tin oxide, ITO) takes place on the coverslip. But if they must be present on both the bottom *and* the cover of the microchannel (as for nDEP), both substrates must be glass, as depicted in Fig. 1. In this case, the microfluidic sandwich consists of a slide with channel walls

from photoresist (with boreholes for the in- and outflow of fluid) and a coverslip, both with microelectrodes on them (Fig. 10). Sealing of the channel is achieved by a layer of silicone rubber that is screen-printed on the channel walls (see Sect. 2.2).

Microelectrode paths are structured by lift-off technology and insulated by plasma coating with SiO_2 , except for the contacting areas. Conductor paths on the glass connect the microelectrodes with contact pads and the latter are contacted in the final sandwich by springs to route the voltage to the microelectrodes (Fig. 10a). Such a setup could be used to handle and sort particles and cells by nDEP, which normally takes place in permanently assembled glass covers (Müller et al. 1999; Duschl et al. 2004). The advantage over the conventional setup is that the reversibly mounted sandwich can be easily cleaned.

We have begun to study the pH-dependent switching of certain polymers in such microsystems. Forisomes are large protein complexes in legumes that protect the plants from the loss of photoassimilates by

blocking injured sieve tubes. Two prolate ellipsoid shapes exist between which forisomes can switch reversibly. The elongated form is 30 μm long and 3 μm thick. Addition of divalent cations (e.g., $>32\text{ nM Ca}^{2+}$) or extreme pH values (less than 4.9 or greater than 9.6) induce a swollen state with a length of 20 μm and a diameter of 7 μm , hence increasing the volume by approx. 350%. Forisomes therefore constitute ATP-independent mechanoproteins (Knoblauch et al. 2003; Knoblauch and Peters 2004) which can switch at least 80 times and generate a pulling force of up to 200 nN along their long axis. This property makes them candidates for switching elements, e.g. microvalves, in micro- or nanofluidic channels.

Forisome switching can be induced by electrotitration, i.e., the electrochemical generation of acid and base by reduction of water at the cathode and its oxidation at the anode. The challenge was to devise a microsystem whose channel is freely accessible to deposit protein and which at the same time integrates microelectrodes. The pH distribution (Fiedler et al. 1995) can be visualized using the pH reporter fluorescein isothiocyanate (FITC). From measurements of the FITC fluorescence as a function of time in the quadrupole shown in Fig. 10b, we estimate the velocity of propagation to be 0.1 mm/s (data not shown).

By applying a low-frequency square wave voltage, an alternating pH pattern can be generated that periodically induces a reversible conformational change of the forisome. The image sequence in Fig. 10b shows the quick and reversible switching of the forisome protein complex during application of such an alternating square wave voltage to two of the electrodes (due to problems with forisome immobilization, this experiment was not performed in a microchannel, but on an open coverslip surface). This demonstrates its possible use as an electrically driven actuator in microfluidic systems. The next step would be to devise a microsystem which is equipped with planar microelectrodes but whose channels are accessible to introduce the protein aggregate, for which the MicCell is well suited.

4 Discussion

We present here a novel microfluidic perfusion system for the microscope whose coverslip is reversibly mounted and whose channel configuration can be freely chosen. The system consists of a computer-controlled, external fluidic system with one to three syringe pumps and/or valves, an invariant channel support, which mediates the installation of a microchannel system into a microscope, and standardized inlets and outlets (UNF fittings) connecting the microchannel with external fluidics. Thus, it provides a highly modular, easy to mount system with a standard interface between microfluidics (of any type and any material) and macrofluidics. To our knowledge, there is no other comparable microscopic

perfusion system on the market that combines all features of our system.

Most applications shown here were realized using PDMS molding, as this is highly valuable in laboratory environments and well suited for rapid prototyping due to its flexibility and ease of use; only a new master for PDMS molding and minor adjustments of the flow control software are needed. We present a novel PDMS casting station that massively simplifies the production of PDMS microchannels and their integration into a microscope setup. In addition, a suggestion is made how one can control biochemical reactions in microchannels by hydrogel valves. Applications and variations of this system are endless.

4.1 Setup options

The fluid transport is constant at high to intermediate flow rates using our current pumps, but smaller syringes or damping loops can be used or the syringe pumps can be exchanged with slower or pulsation-free syringe pumps if slower rates are needed. In general, external syringe pumps are more reliable and generate higher pressure than other methods such as piezoelectric pumps or electroosmosis and provide a higher flexibility because they can be freely arranged. So gentle handling of cells, organelles, micro- or nanobeads, and biomolecules can be achieved—but also the handling of aggressive chemicals, since no metals come in contact with the fluid.

Although our channel system is preferentially made of PDMS because it is easy to fabricate and easy to seal against a coverslip, other materials can be used. We have, for example, devised a system in which the PDMS channel plate is replaced by a glass support (with polymer walls) onto which electrodes can be microstructured (see Sect. 3.6). This expands the capability of the MicCell, although here sealing of the channel is slightly more difficult. In addition, ceramics or hot-embossed or injection-molded plastics can be used as fluidic “cartridges,” and it is possible to mold a PDMS microchannel on a coverslip and then clamp this stack into the microscopy cell, thus making possible the observation of opaque objects (through the transparent PDMS layer) in the flow.

PDMS is generally biocompatible, but may cause problems in some cases, especially when high light intensities are involved as in fluorescence imaging. It has been noted that, in addition to photobleaching, the function of microtubules (but not kinesin) decays rapidly in illuminated PDMS channels (Brunner et al. 2004), obviously due to oxygen diffusing through PDMS. We have experienced the same effect, but have no problems in all-glass chambers (data not shown). In this case, other flow cells must be employed: either one uses a glass-polymer-glass sandwich (see Sect. 2.2) or the flow cell is set up with double-faced tape as microchannel wall (i.e., the microchannel is punched out) that

is glued onto a slide with pre-drilled boreholes and capped by a coverslip.

The modularity of the system not only allows rapid prototyping, but also advanced liquid control by either external distribution valves or hydrogel microvalves, both of which can inject reaction partners into the flowthrough channel, albeit with different dead volumes. The hydrogel microvalve can be connected to the sample reservoir via a tube; it can, however, also contain an open reservoir and filled by a pipette; such a system could be integrated into a liquid handling system and would allow screening of, e.g., chemical libraries.

4.2 Applications and outlook

Of the numerous applications, only a few are discussed here. A first example is high-throughput screening using FCS of particle suspensions which are identified on the basis of their fluorescence signals and sorted shortly thereafter. One could easily search for cells containing two labels (Fu et al. 1999; Dittrich and Schwille 2003; Dittrich et al 2004) or for two labels in close vicinity using FRET. Simpler applications would use imaging methods for viability and other physiological tests and the determination of the uniformity of microbeads.

Quite similar would be the handling of microobjects using laser tweezers (Grier 2003) or dielectrophoresis (Müller et al. 1999; Duschl et al. 2004). Cell identification and sorting can also be achieved by the nonspecific but quick identification of cancerous or stem cells in the “optical stretcher” (Fig. 9), which requires two opposing optical fibers that must be aligned to at least 3 μm . By structuring two “funnels” into the PDMS and adding a feeding system for the optical fibers, we were able to reach this accuracy. A useful addition to cell handling which has not yet been tested would be electroporation in the flow. Although not addressed here, an obvious application would be the screening of adherent cells or tissue slices. Cells are grown outside the channel on a coverslip which is then attached to the microchannel. The cells can then be treated with diverse ligands whose binding can be observed.

Immobilization of biomolecules on the microchannel surface is possible by letting them flow through the channel. Flexibility is added by immobilizing them on the coverslip (e.g., using a microarrayer) before assembling the flow chamber. This could be used to study the interaction of cells with immobilized proteins and polysaccharides, e.g., in adhesion assays as described by Alon and Feigelson (2002). Such assays can be augmented when these molecules are immobilized as a gradient. We have shown that the formation of concentration gradients in microchannels and their immobilization on surfaces is feasible (Fig. 8).

Reactions in the MicCell can be started and stopped on time with a hydrogel valve, and hydrodynamic flow fields in different directions can be used for the manip-

ulation of molecules (e.g., DNA, motor proteins, and other fibers) for the bottom-up construction of nanostructures and nanomachines. Another use for such a device would be a miniaturized chamber for chemical synthesis as described by Kobayashi et al. (2004) or a chamber to hybridize cDNA to DNA microarrays or to bind ligands to antibody arrays. Since temperature control is a prerequisite (as for growing cells), microelectrodes can be added to the microsystem, for both heating and temperature sensing. Microelectrodes can also be used for dielectrophoretic manipulation of particles (as described earlier), to control and measure the pH (e.g., to drive biochemical reactions, see Sect. 3.6), micro-capillary electrophoresis under microscopic control, etc.

Higher integration using multiple channels in parallel and automatic injection into hydrogel valves via a liquid handling instrument would add another twist to this device. An interface to standard microscopes might also be possible. And finally, it must be mentioned that a modular micro-flow cell is not only useful for microscopy, but also for other physical methods that work without a microscope, such as surface plasmon resonance and electrochemical detection (e.g., of signals from immobilized heart muscle or nerve cells or other biosensors); experiments in these directions are under way (not shown). We expect that many more aspects will be added to this list in the near future.

Acknowledgements We thank G. Fuhr (Fh-IBMT) and G. Gradl (Evotec Technologies GmbH, Berlin) and their coworkers for cooperation in the field of nDEP and cell sorting, M. Knoblauch (Fh-IME, Aachen) for the supply of forisomes, W. Pompe (TU Dresden) and J. Howard (MPI-CBG Dresden) for useful discussions on nanostructuring, and C. Wenzel and K. Richter (TU Dresden) for their help with ASE. This work was funded by Grants from the German Ministry of Education, Science, Research, and Technology (BMBF) (Grant No. 0314025 and 0314036), the Deutsche Forschungsgemeinschaft (FOR 335), the Saxonian Ministry of Science and Arts (SMWK), and the Sächsische Aufbaubank (SAB) (Grant No. 6988/1099 and 9890/1519).

References

- Allemand JF, Bensimon D, Jullien L, Bensimon A, Croquette V (1997) pH-dependent specific binding and combing of DNA. *Biophys J* 73:2064–2070
- Alon R, Feigelson S (2002) From rolling to arrest on blood vessels: leukocyte tap dancing on endothelial integrin ligands and chemokines at sub-second contacts. *Semin Immunol* 14:93–104
- Andersson H, van den Berg A (2003) Microfluidic devices for cellomics: a review. *Sens Actuators B Chem* 92:315–325
- Böhm KJ, Stracke R, Baum M, Zieren M, Unger E (2000) Effect of temperature on kinesin-driven microtubule gliding and kinesin ATPase activity. *FEBS Lett* 466:59–62
- Braun E, Eichen Y, Sivan U, Ben-Yoseph G (1998) DNA-templated assembly and electrode attachment of a conducting silver wire. *Nature* 391:775–778
- Brunner C, Ernst KH, Hess H, Vogel V (2004) Lifetime of biomolecules in polymer-based hybrid nanodevices. *Nanotechnology* 15:S540–S548

- Cesaro-Tadic S, Dernick G, Juncker D, Buurman G, Kropshofer H, Michel B, Fattinger C, Delamarche E (2004) High-sensitivity immunoassays for tumor necrosis factor α using microfluidic systems. *Lab Chip* 4:563–569
- Dertinger SKW, Chiu DT, Li Jeon N, Whitesides GM (2001) Generation of gradients having complex shapes using microfluidic networks. *Anal Chem* 73:1240–1246
- Dertinger SKW, Jiang X, Li Z, Murthy VN, Whitesides GM (2002) Gradients of substrate-bound laminin orient axonal specification of neurons. *Proc Natl Acad Sci USA* 99:12542–12547
- Diez S, Reuther C, Dinu C, Seidel R, Mertig M, Pompe W, Howard J (2003) Stretching and transporting DNA molecules using motor proteins. *Nano Lett* 3:1251–1254
- Dittrich PS, Schwille P (2003) An integrated microfluidic system for reaction, high-sensitivity detection, and sorting of fluorescent cells and particles. *Anal Chem* 75:5767–5774
- Dittrich PS, Müller B, Schwille P (2004) Studying reaction kinetics by simultaneous FRET and cross-correlation analysis in a miniaturized continuous flow reactor. *Phys Chem Chem Phys* 6:4416–4420
- Dittrich PS, Jahnz M, Schwille P (2005) A new embedded process for compartmentalized cell-free protein expression and on-line detection in microfluidic devices. *ChemBioChem* 6:811–814
- Duschl C, Geggier P, Jäger M, Stelzle M, Müller T, Schnelle T, Fuhr G (2004) Versatile chip-based tools for the controlled manipulation of microparticles in biology using high frequency electromagnetic fields. In: Andersson H, van den Berg A (eds) *Lab-on-chips for cellomics: micro and nanotechnologies for life science*. Springer, Berlin Heidelberg New York
- Eigen M, Rigler R (1994) Sorting single molecules: application to diagnostics and evolutionary biotechnology. *Proc Natl Acad Sci USA* 91:5740–5747
- Elson EL (1988) Cellular mechanics as an indicator of cytoskeletal structure and function. *Annu Rev Biophys Biophys Chem* 17:397–430
- Fiedler S, Hagedorn R, Schnelle T, Richter E, Wagner B, Fuhr G (1995) Diffusional electrotitration: generation of pH gradients over arrays of ultramicroelectrodes detected by fluorescence. *Anal Chem* 67:820–828
- Fu AY, Spence C, Scherer A, Arnold FH, Quake SR (1999) A microfabricated fluorescence-activated cell sorter. *Nat Biotechnol* 17:1109–1111
- Georgiou G (2001) Analysis of large libraries of protein mutants using flow cytometry. *Adv Protein Chem* 55:293–315
- Grier DG (2003) A revolution in optical manipulation. *Nature* 424:810–816
- Guck J, Ananthkrishnan R, Moon TJ, Cunningham CC, Käs J (2000) Optical deformability of soft biological dielectrics. *Phys Rev Lett* 84:5451–5454
- Guck J, Ananthkrishnan R, Mahmood H, Moon TJ, Cunningham CC, Käs J (2001) The optical stretcher: a novel laser tool to micromanipulate cells. *Biophys J* 81:767–784
- Guck J, Schinkinger S, Lincoln B, Wottawah F, Ebert S, Romeyke M, Lenz D, Erickson HM, Ananthkrishnan R, Mitchell D, Käs J, Ulvick S, Bilby C (2005) Optical deformability as inherent cell marker for testing malignant transformation and metastatic competence. *Biophys J* 88:3689–3698
- Hess H, Clemmens J, Qin D, Howard J, Vogel V (2001) Light-controlled molecular shuttles made from motor proteins carrying cargo on engineered surfaces. *Nano Lett* 1:235–239
- Hess H, Howard J, Vogel V (2002a) A piconewton forcemeter assembled from microtubules and kinesins. *Nano Lett* 2:1113–1115
- Hess H, Clemmens J, Howard J, Vogel V (2002b) Surface imaging by self-propelled nanoscale probes. *Nano Lett* 2:113–116
- Howard J (2001) *Mechanics of motor proteins and the cytoskeleton*. Sinauer Associates, Sunderland
- Huang H, Kamm RD, Lee RT (2004) Cell mechanics and mechanotransduction: pathways, probes, and physiology. *Am J Physiol Cell Physiol* 287:C1–C11
- Knoblauch M, Peters WS (2004) Forisomes, a novel type of Ca^{2+} -dependent contractile protein motor. *Cell Motil Cytoskeleton* 58:137–142
- Knoblauch M, Noll GA, Müller T, Prüfer D, Schneider-Hüther I, Scharner D, van Bel JE, Peters WS (2003) ATP-independent contractile proteins from plants. *Nat Mater* 2:600–603
- Kobayashi J, Mori Y, Okamoto K, Akiyama R, Ueno M, Kitamori T, Kobayashi S (2004) A microfluidic device for conducting gas-liquid-solid hydrogenation reactions. *Science* 304:1305–1308
- Lärmer F, Schilp A (1994) Method of anisotropically etching silicon. US Patent No. 5501893, German Patent DE4241045
- Larson RG, Perkins TT, Smith DE, Chu S (1997) Hydrodynamics of a DNA molecule in a flow field. *Phys Rev E* 55:1794–1797
- Li Jeon N, Dertinger SKW, Chiu DT, Choi IS, Stroock AD, Whitesides GM (2000) Generation of solution and surface gradients using microfluidic systems. *Langmuir* 16:8311–8316
- Lincoln B, Erickson HM, Schinkinger S, Wottawah F, Mitchell D, Ulvick S, Bilby C, Guck J (2004) Deformability-based flow cytometry. *Cytometry* 59A:203–209
- Lipman EA, Schuler B, Bakajin O, Eaton WA (2003) Single-molecule measurement of protein folding kinetics. *Science* 301:1233–1235
- Madge D, Elson E, Webb WW (1972) Thermodynamic fluctuations in a reacting system—measurement by fluorescence correlation spectroscopy. *Phys Rev Lett* 29:705–708
- Manz A, Graber N, Widmer HM (1990) Miniaturized total chemical analysis systems: a novel concept for chemical sensing. *Sens Actuators B Chem* 1:244–248
- Manz A, Fetting JC, Verpoorte E, Lüdi H, Widmer HM, Harrison DJ (1991) Micromachining of monocrystalline silicon and glass for chemical analysis systems: a look into next century's technology or just a fashionable craze? *Trends Anal Chem* 10:144–149
- Maubach G, Csáki A, Seidel R, Mertig M, Pompe W, Born D, Fritzsche W (2003) Controlled positioning of a DNA molecule in an electrode setup based on self-assembly and microstructuring. *Nanotechnology* 14:1055–1056
- Mertig M, Pompe W (2004) Biomimetic fabrication of DNA-based metallic nanowires and networks. In: Niemeyer CM, Mirkin CA (eds) *Nanobiotechnology: concepts, applications and perspectives*. Wiley-VCH, Weinheim, pp 256–277
- Mertig M, Colombi Ciacchi L, Seidel R, Pompe W, De Vita A (2002) DNA as a selective metallization template. *Nano Lett* 2:841–844
- Müller T, Gradl G, Howitz S, Shirley S, Schnelle T, Fuhr G (1999) A 3-D microelectrode system for handling and caging single cells and particles. *Biosens Bioelectron* 14:247–256
- Pompe T, Zschoche S, Herold N, Salchert K, Gouzy MF, Sperling C, Werner C (2003) Maleic anhydride copolymers—a versatile platform for molecular biosurface engineering. *Biomacromolecules* 4:1072–1079
- Prots I, Stracke R, Unger E, Böhm KJ (2003) Isopolar microtubule arrays as a tool to determine motor protein directionality. *Cell Biol Int* 27:251–253
- Richter J, Mertig M, Pompe W, Mönch I, Schackert HK (2001) Construction of highly conductive nanowires on a DNA template. *Appl Phys Lett* 78:536–538
- Richter A, Kuckling D, Howitz S, Gehring T, Arndt KF (2003) Electronically controlled microvalves based on smart hydrogels: magnitudes and potential applications. *J Microelectromech Syst* 12:748–753
- Richter A, Howitz S, Kuckling D, Arndt KF (2004) Influence of volume phase transition phenomena on the behavior of hydrogel-based valves. *Sens Actuators B Chem* 99:451–458
- Ruardy TG, Schakenraad JM, van der Mei HC, Busscher HJ (1997) Preparation and characterization of chemical gradient surfaces and their application for the study of cellular interaction phenomena. *Surf Sci Rep* 29:3–30

- Schinkinger S, Wottawah F, Travis KA, Lincoln B, Guck J (2004) Feeling for cells with light. *Proc SPIE Optical Trapping Optical Micromanipulation* 5514:170–178
- Schnapp BJ, Crise B, Sheetz MP, Reese TS, Khan S (1990) Delayed start-up of kinesin-driven microtubule gliding following inhibition by adenosine 5'-[beta,gamma-imido]triphosphate. *Proc Natl Acad Sci USA* 87:10053–10057
- Scholey JM (1993) Motility assays for motor proteins (*Methods in cell biology*, vol 39). Academic Press, San Diego
- Seeman NC (1996) The design and engineering of nucleic acid nanoscale assemblies. *Curr Opin Struct Biol* 6:519–526
- Stracke P, Böhm KJ, Burgold J, Schacht HJ, Unger E (2000) Physical and technical parameters determining the functioning of a kinesin-based cell-free motor system. *Nanotechnology* 11:52–56
- Van Vliet KJ, Bao G, Suresh S (2003) The biomechanics toolbox: experimental approaches for living cells and biomolecules. *Acta Materialia* 51:5881–5905
- Wirtz D (1995) Direct measurement of the transport properties of a single DNA molecule. *Phys Rev Lett* 75:2436–2439
- Wottawah F, Schinkinger S, Lincoln B, Ananthakrishnan R, Romeyke M, Guck J, Käs J (2005) Optical rheology of biological cells. *Phys Rev Lett* 94:098103
- Yan H, Park SH, Finkelstein G, Reif JH, LaBean T (2003) DNA-templated self-assembly of protein arrays and highly conductive nanowires. *Science* 301:1882–1884
- Zimmermann RM, Cox EC (1994) DNA stretching on functionalized gold surfaces. *Nucleic Acids Res* 22:492–497